Low temperature capture of open shell dipolar molecules by ions: the capture of rotationally selected NO($^2\Pi_{1/2}$, j) by C$^+$

E. I. Dashevskaya,[ab] I. Litvin,[ac] E. E. Nikitin[ab] and J. Troe*[bc]

The low-energy capture of dipolar diatomic molecules in an open electronic state by ions is usually considered to be induced by the first-order charge–permanent dipole interaction with other terms of the long-range potential playing a minor role. If the molecular dipole moment is anomalously small (as is the case for slightly asymmetrical molecules), however, the situation changes, and the capture dynamics is strongly affected by higher orders of the charge–permanent dipole, charge–permanent quadrupole, and charge–induced dipole interactions. The interplay of different terms in the interaction potential manifests itself in complicated temperature dependence of the rotationally state-specific capture rate coefficients. These features of the capture are studied by way of example for NO(X $^2\Pi_{1/2}$, j) + C$^+$ collisions in the temperature range 10^{-2}–20 K where the dynamics is adiabatic with respect to rotational and fine-structure transitions and sudden with respect to transitions between Λ doubling and hyperfine states. The theoretical rate coefficient, which depends on the translational and rotational temperature, agrees with the experimental one measured at T_{tr} = 0.6 K and T_{rot} = 20 K.

1. Introduction

Capture of diatomic molecules by ions at low temperatures (energies) occurs adiabatically with respect to rotational transitions $j \rightarrow j'$ and transitions between close-lying electronic states (e.g. fine-structure transitions $\Omega \rightarrow \Omega'$ within a given electronic manifold $^{2S+1}\Lambda_\Omega$) (for the latest reviews, see, e.g. ref. 1 and 2). Under these conditions, the capture dynamics in the adiabatic roronic (rotational + electronic) basis is described by a set of coupled wave equations for states that arise from the free Ω, j, m states.[3] The numerical solution of the capture equations (scattering equations with absorbing boundary conditions on the complex surface) does not require much computational effort for each particular case that is specified by a set of parameters which characterize the long-range part of the molecule–ion interaction potential. An implicit assumption within this approach is that the capture dynamics corresponds to the sudden limit with respect to transitions between energy levels which correspond to Λ doubling and hyperfine interactions.[4] However, the condition of sudden dynamics with respect to the latter interaction is too demanding if the initial population of asymptotic close-lying levels is statistical and if one is interested in the calculation of the capture rate coefficient from all these states rather than from individual ones: in this case, deviations from sudden dynamics will not show up, even for values of the Massey parameter which are not small. Thus the two conditions, a large value of the Massey parameter for rotational transitions

and a small value of the energy spacing between the Λ doubling and hyperfine energy levels compared to kT, leave a wide temperature range within which the capture can be treated adiabatically with respect to different rotational states, while the existence of Λ doubling and hyperfine states can be ignored altogether. For the capture of NO(X $^2\Pi_{1/2}$, j) by C$^+$ ions, with a rotational constant of NO of about 1.7 cm^{-1} and with Λ doubling and hyperfine splitting of about 0.01 cm^{-1} and 0.001 cm^{-1},[5] respectively, the temperature range in question extends roughly from 10^{-2} to 20 K. We emphasize again that the major difference between the capture dynamics of molecules in a degenerate vs. closed electronic state is the first-order Stark interaction with an ion for the former case in the region important for the capture. With a decrease in temperature, this region moves to larger interfragment separation where the first-order Stark effect becomes the second-order one. The detailed study of this transition, discussed qualitatively in ref. 4, is beyond the scope of this work and is the subject of a future publication.[6]

The aim of the present paper is to study capture dynamics and calculate the state-specific rate coefficients for the capture of NO(X $^2\Pi_{1/2}$, j) in different rotational states by a C$^+$ ion within the above given temperature range. Our interest in this process arose from the following observations:

(i) The small dipole moment of NO results in the interesting manifestation of different types of long-range interaction terms in the capture dynamics even at low temperatures. This was noted earlier for the ground rotational state $j = 1/2$ [7] and is expected to be more pronounced for excited rotations due to the progressively decreasing first-order contribution of the charge–permanent dipole interaction for increasing j.

(ii) The temperature range indicated, i.e. say, 0.02–20 K, includes the characteristic rotational temperature of NO, $\theta_{rot} = B/k$ = 2 K, with B being the rotational constant of

^{a} Schulich Faculty of Chemistry, Technion-Israel Institute of Technology, Haifa, 32000, Israel
^{b} Max-Planck-Institut für Biophysikalische Chemie, Am Fassberg, D-37077 Göttingen, Germany
^{c} Institut für Physikalische Chemie der Universität Göttingen, Tammannstrasse 6, D-37077 Göttingen, Germany

NO molecule in energy units; this provides the opportunity to study the applicability of the perturbed rotor (PR) approximation, believed to be valid at $T \ll \theta_{\mathrm{rot}}$. The latter, in turn, can be written in different approximations, neglecting or including the second-order correction stemming from the charge–permanent dipole interaction. One can expect that with a small value of the rotational constant of NO, the second-order correction may be quite significant. In this case, this effect will be similar to that for molecules in the Σ state.[8]

(iii) There exist experimental data for the capture of NO(X $^2\Pi_{1/2}$, j) by C$^+$ ions.[7] We feel that the earlier interpretation of these from ref. 7 requires some revision which is based on a more accurate interaction potential and which includes contributions from excited rotational states of NO.

The long-range interaction between an ion and a dipolar, quadrupolar and polarizable molecule in a degenerate electronic state includes too many parameters to allow for a meaningful general formulation of the capture rate. Indeed, if the potential is written as an expansion in powers of $1/R$ up to the $1/R^4$ term, the number of parameters is five (one for the charge–permanent dipole term, two for the charge–permanent quadrupole term, and two for the anisotropic charge–induced dipole term). The adiabatic potentials for an isolated Ω state will include one more parameter, the rotational constant of the diatom. The total number of six parameters then appears to be too large for use in the construction of a general picture of the dependence of the capture rate coefficient on the potential on the basis of a numerical solution of the capture problem. Because of this complicated situation, we restrict ourselves to a case study only, *i.e.* to the capture of NO by C$^+$.

In the attempt to draw a general picture, one usually introduces approximations of dynamic (equations of motion) and static (interaction) character. The former frequently consists of replacing the quantum equations for the relative motion by their classical counterparts and adopting the adiabatic channel (AC) approximation, while the latter introduces certain simplifications in the interaction potential (*e.g.* the neglect of the anisotropy of the charge–induced dipole term and the use of one, instead of two, quadrupole moments). In this paper, we discuss these approximations with reference to the NO(X $^2\Pi_{1/2}$, j) + C$^+$ system.

The plan of our presentation is as follows. Section 2 outlines the general expressions for the interaction energy, the adiabatic-channel potentials, and the rate coefficients. Section 3 describes calculations of the rate coefficients for NO(X $^2\Pi_{1/2}$, $j = 1/2$) + C$^+$ capture for PR and accurate AC potentials and presents simple estimations of quantum corrections to the classical treatment. In Section 4 state-specific rate coefficients for $j > 1/2$ are discussed and the two-temperature (different translational and rotational temperatures) rate coefficients are calculated. Section 5 compares the theoretical rate coefficient with an experimental value.

2. Interaction energy, adiabatic-channel potentials and rate coefficients

If one ignores the hyperfine interaction, the wave function of a low-lying roronic state of NO is represented by a main term that corresponds to the electronic nomenclature $^2\Pi_{1/2}$ of the

Hund coupling case a, the correction term $^2\Pi_{3/2}$ and a very small correction term $^2\Sigma$.[10] The interaction responsible for the correction term slightly modifies the pattern of roronic energy levels for the pure Hund coupling case a, provided that $B(j + 1/2) \ll A$ where A is the spacing between the levels of the non-rotating molecule in its ground state, $^2\Pi_{1/2}$, and its low-lying excited state, $^2\Pi_{3/2}$. For this pattern, each roronic level is doubly degenerate. This degeneracy is lifted by the very small interaction with the $^2\Sigma$ state resulting in the Λ doubling. Dynamically, the splitting of the Λ doublet can be neglected provided that the associated Massey parameter is small. This condition imposes a lower limit for the temperature at which the Λ doublet phenomenon can be disregarded.

In this paper, the energy levels of a free NO molecule and the AC potentials were calculated assuming that the states of the free molecule belong to the pure coupling case a. Therefore, the rotating NO molecule in its ground electronic state X $^2\Pi_{1/2}$ is modelled by a symmetric rotor with fixed values $\tilde{\Omega}$ of the projection of the intrinsic angular momentum j onto the molecular axis, $\tilde{\Omega} = \pm 1/2$. The long-range part of the ion–molecule interaction potential V is written in the form which accounts for the fact that the quadrupole tensor for a state Ω $|\tilde{\Omega}| = 1/2$ is axially symmetric and which neglects the small anisotropy in the charge–induced dipole term. As a result, the charge–permanent quadrupole term contains only one parameter and the charge–induced dipole term becomes spherically symmetric. In this way we have:

$$V(R, \gamma) = \frac{q\boldsymbol{\mu}_{\mathrm{D}}}{R^2} P_1(\cos\gamma) + \frac{q\boldsymbol{Q}}{R^3} P_2(\cos\gamma) - \frac{q^2\boldsymbol{\alpha}}{2R^4} \qquad (1)$$

where R is the distance between the ion and the centre-of-mass the diatom and γ is the angle between the collision axis $\boldsymbol{R}$ (directed from the centre-of-mass of the diatom toward the ion) and the molecular axis $\boldsymbol{r}$ (directed along the dipole moment vector), P_1 and P_2 are the Legendre polynomials, $\boldsymbol{\mu}_D$, $\boldsymbol{Q}$, $\boldsymbol{\alpha}$ are the dipole moment, quadrupole moment, and mean polarizability of the diatom, respectively, and q is the charge of the ion.

The interaction potential $V(R, \gamma)$ in eqn (1) gives rise to AC potentials. The latter are defined as the eigenvalues of the AC matrix generated from the potential in eqn (1) and the rotational energy of the diatom $E_{j,\tilde{\Omega}} = Bj(j + 1)$ in the basis of free rotor functions of the diatom with the collision axis taken as the quantization axis for the intrinsic angular momentum.[11] Within this approach, the AC matrix is diagonal in $\tilde{\Omega}$ (the projection of $\boldsymbol{j}$ onto molecular axis) and $\tilde{\omega}$ (the projection of $\boldsymbol{j}$ onto the collision axis). The eigenvalues of this matrix are labelled, beside $\tilde{\Omega}$ and $\tilde{\omega}$, by a quantum number $\tilde{j}$. Since $\tilde{j}$ can unambiguously be related to j by adiabatic correlation, the eigenvalues can also be labelled by $j, \tilde{\Omega}, \tilde{\omega}$, and written as $^{\mathrm{AC}}V_{j,\tilde{\Omega}\tilde{\omega}}(R)$ (in the following text, we will not use superscript AC in all cases where it does not lead to ambiguities). If the basis of the free rotor functions is large enough to ensure the convergence at those interfragment separations which are important for the capture, we consider the eigenvalues of the AC matrix to be accurate and denote them as $V^{\mathrm{acc}}_{j,\tilde{\Omega},\tilde{\omega}}(R)$. In this work, we have calculated accurate AC potentials for the system NO$^+$ with interaction parameters such as those used in ref. 7 and listed in Table 1.

Table 1 Interaction parameters for the NO (X $^2\Pi$) molecule

A_{so}	124.2 cm^{-1}	= 5.66 × 10^{-4} a.u.
B_{rot}	1.7046 cm^{-1}	= 7.77 × 10^{-6} a.u.
$\boldsymbol{\mu}_D$	0.160 D	= 0.06295 a.u.
$\boldsymbol{Q}$	−2.421 × 10^{-26} esu cm^2	= −1.80 a.u.
$\boldsymbol{\alpha}$	1.680 × 10^{-24} cm^3	= 11.337 a.u.

As an approximation to $V^{acc}_{j,\tilde{\Omega},\tilde{\omega}}(R)$ in the low-energy regime, one can take the expansion of $V^{acc}_{j,\tilde{\Omega},\tilde{\omega}}(R)$ in powers of $1/R$ up to the term $1/R^4$. This expansion, called the perturbed rotor (PR) or weak-field approximation, reads[12]

$$V^{PR}_{j,\tilde{\Omega},\tilde{\omega}}(R) = E_{j,\tilde{\Omega}} - \frac{\tilde{\omega}q\boldsymbol{\mu}_D\tilde{\Omega}}{j(j+1)}\frac{1}{R^2} + \frac{q\boldsymbol{Q}(j(j+1)-3\tilde{\omega}^2)}{(2j+3)(2j-1)}$$

$$\times \frac{(j(j+1)-3\tilde{\Omega}^2)}{j(j+1)}\frac{1}{R^3} + -\frac{\boldsymbol{\alpha}q^2}{2}\frac{1}{R^4} + \frac{\boldsymbol{\mu}_D^2q^2}{2B}$$

$$\times \left(\frac{(j^2-\tilde{\Omega}^2)(j^2-\tilde{\omega}^2)}{j^3(2j-1)(2j+1)} - \frac{((j+1)^2-\tilde{\Omega}^2)((j+1)^2-\tilde{\omega}^2)}{(j+1)^3(2j+1)(2j+3)}\right)\frac{1}{R^4}$$

(2)

Approximations to eqn (2), to be referred to later in this paper, are a truncated version of PR (TPR) (neglecting the second-order charge–dipole correction in brackets) and a version taking into account only the first-order charge–permanent dipole (CD) interaction.

To avoid unnecessary complications arising from different combinations of the two quantities $\tilde{\Omega},\tilde{\omega}$, we introduce new quantum numbers, the absolute value of the projection $\Omega = |\tilde{\Omega}| = 1/2$ and $m = \pm|\tilde{\omega}|$, with the signs + and − corresponding to the lower and upper states of the same value of $|\tilde{\omega}|$, respectively. Then $V^{PR}_{j,\tilde{\Omega},\tilde{\omega}}(R)$ will be rewritten as $V^{PR}_{j,m}(R)$ and eqn (2), with $\Omega = 1/2$, assumes the form

$$V^{PR}_{j,m}(R) = E_{j,\Omega} \mp \frac{mq\boldsymbol{\mu}_D}{2j(j+1)}\frac{1}{R^2} + \frac{q\boldsymbol{Q}(j(j+1)-3m^2)}{(2j+3)(2j-1)}$$

$$\frac{(j(j+1)-3/4)}{j(j+1)}\frac{1}{R^3} - \frac{\boldsymbol{\alpha}q^2}{2}\frac{1}{R^4} + \left[\frac{\boldsymbol{\mu}_D^2q^2}{2B}\left(\frac{(j^2-1/4)(j^2-m^2)}{j^3(2j-1)(2j+1)}\right.\right.$$

$$\left.\left. - \frac{((j+1)^2-1/4)((j+1)^2-m^2)}{(j+1)^3(2j+1)(2j+3)}\right)\right]\frac{1}{R^4}$$

(3)

The AC potentials $V^{PR}_{j,m}(R)$ and $V^{acc}_{j,m}(R)$ generate effective radial potentials $U^{PR}_{J,j,m}(R)$ and $U^{acc}_{J,j,m}(R)$ that drive the motion of colliding partners towards the complex boundary in a state with a fixed value of the total angular momentum quantum number J. There are different ways to define the effective potentials.[11] The most consistent way is to supplement $V^{acc}_{j,m}(R)$ with the expectation value of the centrifugal energy in the J, j, m state:

$$U^{acc}_{J,j,m}(R) = \left\langle Jjm\left|\frac{(\hat{\boldsymbol{J}}\cdot\hat{\boldsymbol{j}})^2}{2\mu R^2}\right|Jjm\right\rangle + V^{acc}_{j,m}(R)$$

(4)

Note that in eqn (4) $\hat{\boldsymbol{j}}$ is the operator of the intrinsic angular momentum, but j is not the quantum number that is associated with $\hat{\boldsymbol{j}}$ since it has only asymptotic significance. In the PR approximation, j is the quantum number that is associated

with $\hat{\boldsymbol{j}}$. The first term on the r.h.s. of eqn (4) can then be written explicitly, and we get

$$U^{PR}_{J,j,m}(R) = \frac{\hbar^2}{2\mu R^2}(J(J+1) - 2m^2 + j(j+1)) + V^{PR}_{j,m}(R)$$

(5)

In the classical approximation, when J is regarded as large ($J \gg j$) and continuous, the relative rotational energies in the acc and PR approximation become the same, and the effective potentials are written as

$$U_{j,m}(R,J) = \frac{\hbar^2 J^2}{2\mu R^2} + V_{j,m}(R)$$

(6)

where the superscript PR can be added to indicate the PR approximation.

The general expression for the partial AC rate coefficient finally is given by

$$k_{j,m}(T) = \sqrt{\frac{8kT}{\pi\mu}}\sum_{J\geq|m|}^{\infty}\frac{\pi\hbar^2}{(2j+1)2\mu kT}$$

$$\times \int_0^{\infty}(2J+1) \times P_{J,j,m}(E)\exp(-E/kT)\frac{dE}{kT}$$

(7)

where $P_{J,j,m}(E)$ is the AC capture probability for the channel J, j,m. The additional superscript PR, when needed, can be added. The classical rate coefficient is derived from eqn (7) when the summation over J is replaced by integration, and the probability $P_{J,j,m}(E)$ is replaced by the step function $\Theta(E - U^{max}_{j,m}(J))$. Here $U^{max}_{j,m}(J)$ is the maximal value of $U^{max}_{j,m}(R;J)$ with respect to R, if a maximum exists; otherwise, one should put $U^{max}_{j,m}(J)$ equal to zero. In this way, the classical version of eqn (7) reads

$$k_{j,m}(T) = \sqrt{\frac{8kT}{\pi\mu}}\int_0^{\infty}\frac{\pi\hbar^2 JdJ}{(2j+1)\mu kT}\exp(-U^{max}_{j,m}(J)/kT)$$

(8)

The total rate coefficient is represented as the sum of partial rate coefficients:

$$k_j(T) = \sum_{m=-j}^{j}k_{j,m}(T)$$

(9)

3. Capture of NO(X $^2\Pi_{1/2}$, $j = 1/2$) by C$^+$: perturbed rotor and accurate AC potentials

Perturbed rotor potentials

The PR potentials as derived from eqn (3) read:

$$V^{PR}_{1/2,m}(R) = -\frac{2m\boldsymbol{\mu}_D q}{3R^2} - \frac{q^2\boldsymbol{\alpha}^{PR}}{2R^4}$$

(10)

with the effective PR polarizability $\boldsymbol{\alpha}^{PR} = \boldsymbol{\alpha} + (4/27)\boldsymbol{\mu}_D^2/B$. Along with the PR potential from eqn (3), we will also consider the truncated PR (TPR) potential

$$V^{TPR}_{1/2,m}(R) = -\frac{2m\boldsymbol{\mu}_D q}{3R^2} - \frac{q^2\boldsymbol{\alpha}}{2R^4}$$

(11)

This journal is © the Owner Societies 2007

Phys. Chem. Chem. Phys., 2007, **9**, 1559–1567 | 1561

in which the second-order correction to the $1/R^4$ term is neglected. The potential $V_{1/2,1/2}^{PR}$ is purely attractive while $V_{1/2,-1/2}^{PR}$ passes through a maximum $V_{1/2,-1/2}^{PR,max} \equiv E_{1/2,-1/2}^{*PR} = \mu_D^2/18\alpha^{PR}$. The AC potentials $V_{1/2,m}^{PR}(R)$ in eqn (10) define the effective ACCl potentials $U_{1/2,m}^{PR}(R,J)$ according to eqn (4). The potentials $V_{1/2,1/2}^{PR}(R,J)$ are purely attractive for $J < \tilde{J}_c$ and possess maxima for $J < \tilde{J}_c$ where $\tilde{J}_c^2 = 2\mu\mu_D q/3\hbar^2$, while the potentials $U_{1/2,-1/2}^{PR}(R)$ possess maxima for all J. The maximal values of the effective AC potentials are

$$U_{1/2,1/2}^{max}(J) = \frac{\hbar^4(J^2 - \tilde{J}_c^2)^2}{8\mu^2 q^2 \alpha^{PR}}, J \geq \tilde{J}_c;$$

$$U_{1/2,-1/2}^{max}(J) = \frac{\hbar^4(J^2 + \tilde{J}_c^2)^2}{8\mu^2 q^2 \alpha^{PR}}, J \geq 0 \qquad (12)$$

Thus the general expression for the rate coefficient $k_{1/2}^{PR}$ can be written as

$$k_{1/2}^{PR}(T) = k_{1/2,1/2}^{PR}(T) + k_{1/2,-1/2}^{PR}(T) \qquad (13)$$

Here, the partial rate coefficients are

$$k_{1/2,1/2}^{PR}(T) = \frac{1}{6}\mu_D q\sqrt{\frac{8\pi}{\mu kT}} + \pi q\sqrt{\frac{\alpha^{PR}}{\mu}} \qquad (14)$$

$$k_{1/2,-1/2}^{PR}(T) = \pi q\sqrt{\frac{\alpha^{PR}}{\mu}}\text{erfc}\left(\sqrt{E_{1/2,-1/2}^{*PR}/kT}\right) \qquad (15)$$

where $\text{erfc}(x)$ is the complementary error function, $\text{erfc}(x) = (2/\pi)\int_x^\infty \exp(-y^2)\,dy$.

If eqn (13)–(15) are rewritten for the reduced rate coefficient $\chi_{PRL}^{PR} = k^{PR}/k_{PRL}$ with $k_{PRL} = 2\pi q\sqrt{\alpha^{PR}/\mu}$ being the Langevin capture rate coefficient for the PR potential $-q^2\alpha^{PR}/2R^4$, then χ_{PRL}^{PR} is found to depend on a single variable, i.e. on the reduced temperature $\theta^{PR} = kT/E_{1/2,-1/2}^{*PR}$. It then is given by

$$\chi_{PRL}^{PR}(\theta^{PR}) = k^{PR}/k_{PRL} = 1\big/\sqrt{\pi\theta^{PR}} + 1/2$$
$$+ (1/2)\,\text{erfc}(1\big/\sqrt{\theta^{PR}}) \qquad (16)$$

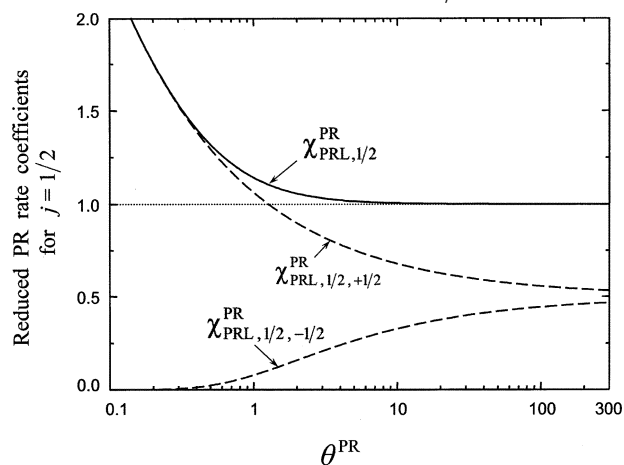**Fig. 1** Reduced total (full line, $\chi_{PRL,1/2}^{PR}$) and partial (dashed lines, $\chi_{PRL,1/2,+1/2}^{PR}$, $\chi_{PRL,1/2,-1/2}^{PR}$) PR rate coefficients for capture in the $j = 1/2$ state vs. reduced temperature θ^{PR}, see text. The dotted horizontal line is drawn for orientation.

The plot of χ_{PRL}^{PR} and its partial contributions vs. θ^{PR} is shown in Fig. 1. The low-temperature limit of χ_{PRL}^{PR} corresponds to the capture for the first-order charge–permanent dipole potential, and the high-temperature limit to the capture for the charge–induced dipole + second-order charge–permanent dipole potential. The value of the ACCl-PR capture rate constant at this limit, $k_{1/2}^{PR} \to k_{PRL} = 2\pi q\sqrt{\alpha^{PR}/\mu}$, is higher than expected for the general potential of eqn (1) which predicts that the high-temperature limit corresponds to the capture for the charge–induced dipole potential, $k_{1/2} \to k_L = 2\pi q\sqrt{\alpha/\mu}$. This discrepancy is explained by the inadequacy of the second-order charge–permanent dipole correction at very high temperatures. The extent of this discrepancy beyond the second-order treatment cannot be accomplished in general form. Therefore, in the following we use the specific case of the capture of NO by C^+.

The condition for the applicability of the PR approximation can be formulated as a requirement that the height of the lowest potential barrier in the set of effective potentials $U_{1/2,1/2}^{PR}(R, J)$, $U_{1/2,-1/2;lowest}^{PR,\,max}(J)$ should be substantially smaller than the thermal energy, i.e. $U_{1/2,-1/2;lowest}^{PR,\,max}(J) \ll kT$. The upper value of $U_{1/2,-1/2;lowest}^{max}(J)$ is found from eqn (12) with J exceeding $\tilde{J}_c$ by 1. Putting $J = \tilde{J}_c + 1$ and assuming that $\tilde{J}_c \gg 1$ we write the condition for the classical approximation to apply as

$$\frac{\hbar^4 \tilde{J}_c^2}{2\mu^2 q^2 \alpha^{PR}} \ll kT \qquad (17)$$

Note that the inequality in eqn (17) with $\tilde{J}_c = 1$ corresponds to the condition of applicability of the classical approximation in the calculation of the capture rate coefficient for a potential $-q^2\alpha^{PR}/2R^4$.[13] We thus see that, with $\tilde{J}_c \gg 1$ which is the case for NO($X\,^2\Pi_{1/2}, j = 1/2$) by C^+ collisions, $\tilde{J}_c = 25.62$, the classical approximation for the capture in the field of the potential of eqn (10) is expected to be invalid at substantially higher temperatures than for a pure potential $-q^2\alpha^{PR}/2R^4$. However, the temperature at which the inequality in eqn (17) becomes marginal (about 10^{-4} K for NO + C^+ collisions), is substantially lower than that at which the Λ-doubling effects may manifest themselves. Therefore, within the temperature range under discussion, the classical approximation for the relative motion is adequate.

However, there exists a quantum correction that survives up to relatively high temperatures. It comes from the deviation of the number of quantum capture states from its classical counterpart for purely attractive effective potentials. The correction factor to the first term on the r.h.s. of eqn (14) $f(J_c, \tilde{J}_c)$ will read

$$f(J_c, \tilde{J}_c) = \frac{\sum_{J=1/2}^{J_c}(2J+1)}{\int_0^{\tilde{J}_c} 2J\,dJ} = \frac{(J_c+1/2)(J_c+3/2)}{\tilde{J}_c^2} \qquad (18)$$

where J_c, is the highest quantum number for which $U_{j,m}^{PR}(R,J)$ is attractive. As follows from eqn (5) with $V_{j,m}^{PR}(R)$ corresponding to the first-order charge–permanent dipole interaction, $V_{j,m}^{PR}(R) = V_{j,m}^{CD}(R)$, J_c is defined as $J_c = \text{int}(\tilde{J}_c) - 1/2$. For values of $\tilde{J}_c = 25.62$, $J_c = 24.5$ as appropriate for the case under study, we see that this effect decreases the classical rate only by 1%.
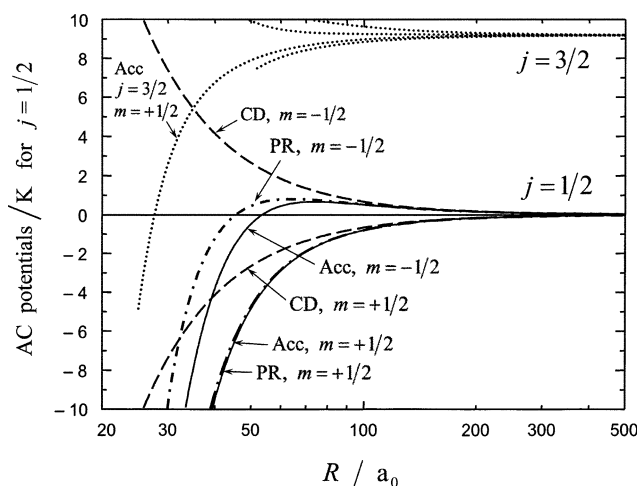
Fig. 2 AC potentials for $NO(^2\Pi_{1/2}, j = 1/2)$ + positive ion in different AC approximations: first-order charge–dipole potentials (CD, dashed lines), perturbed rotor potentials (PR, dash-dotted lines) and accurate potentials (Acc, full lines). The dotted curves correspond to the AC potentials that converge to the limit $j = 3/2$; they are drawn for orientation.

Fig. 3 Reduced total and partial (for purely attractive AC potentials) capture rate coefficients for $NO(^2\Pi_{1/2}, j = 1/2)$ + C^+ for accurate (full lines, $\chi_{L,1/2}$, $\chi_{L,1/2,+1/2}$), PR (dashed lines, $\chi^{PR}_{L,1/2}$, $\chi^{PR}_{L,+1/2}$) and TPR (dotted lines, $\chi^{PR}_{L,1/2}$, $\chi^{TPR}_{L,+1/2}$) potentials. The curve $\chi_{L,1/2,+1/2}$ (see eqn (23)) is equal to χ^{WSC} such as that calculated in ref. 5, see text.

Accurate potentials

The accurate and PR AC potentials for the $NO(X\ ^2\Pi_{1/2}, j = 1/2)$ + ion system, are shown in Fig. 2. In order to illustrate the spacing between the ground and first excited state, the AC potentials for the pure first-order charge–permanent dipole interaction are also shown here, and the accurate potentials that originate from the state $j = 3/2$. We see that the coupling between the ground and excited states hardly affects the PR potential for $m = 1/2$, while it noticeably modifies the potential barrier in the PR potential for $m = -1/2$ (see also Table 2). Once the potentials $V_{1/2,m}(R)$ are known, the calculation of the rate coefficient is straightforward.

Fig. 3 shows the reduced rate coefficients $\chi_L = k/k_L$ for AC potentials determined in different approximations. The dashed curves for $\chi^{PR}_{L,1/2}$, $\chi^{PR}_{L,1/2,1/2}$ are basically identical to $\chi^{PR}_{PRL,1/2}$, $\chi^{PR}_{PRL,1/2,1/2}$ as in Fig. 1 if one takes into account that the normalization of the reduced rate coefficients in the two figures is different. Deviations of $\chi^{PR}_{L,1/2}$, $\chi^{PR}_{L,1/2,1/2}$ from their accurate counterparts $\chi_{L,1/2}$, $\chi_{L,1/2,1/2}$ come from the difference between accurate and PR potentials: the relation $\chi_{L,1/2} > \chi^{PR}_{L,1/2}$ in the range $1 < T < 10$ K is due to the difference in the activation energies $E^*_{1/2,-1/2} < E^{*PR}_{1/2,-1/2}$, while the reverse relation, $\chi_{L,1/2} > \chi^{PR}_{L,1/2}$ above $T = 30$ K is ascribed to the overestimation of the charge–permanent dipole attraction in second-order approximation. At higher temperatures, $\chi_{L,1/2}$ for the adopted interaction potential will converge to unity. Also shown in Fig. 3 are two plots $\chi^{TPR}_{L,1/2}$, $\chi^{TPR}_{L,1/2,1/2}$ for the TPR potential. We see that both $\chi_{L,1/2}$ and $\chi^{PR}_{L,1/2}$ are noticeably higher than $\chi^{TPR}_{L,1/2}$. The implication of this observation will be discussed in section 5.

4. Capture of $NO(X\ ^2\Pi_{1/2}, j > 1/2)$ by C^+: accurate AC potentials

State-specific capture rate coefficients

For $j > 1/2$, the perturbed rotor potential in eqn (4) includes the contribution from the first-order charge–quadrupole inter-
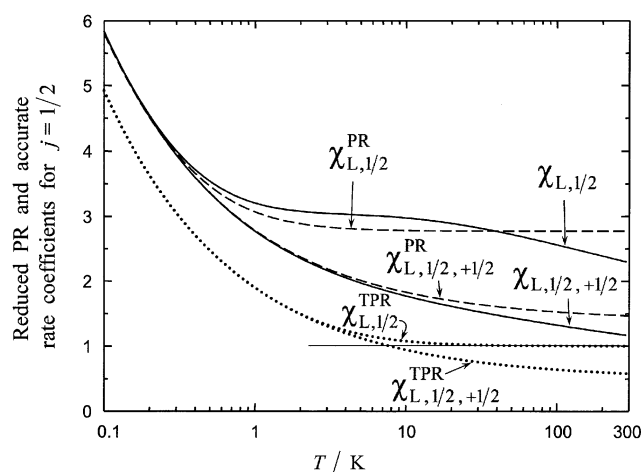
action which affects the pattern of the AC curves and makes an easy analytical treatment impossible. Moreover, the PR approximation may turn out to be inadequate due to the early breakdown of the weak-field expansion.

The PR and accurate AC potentials for $j = 3/2$ are shown in Fig. 4 and the potential barriers are listed in Table 2. We see that the PR approximation predicts that AC potentials with $m = 1/2$ and $m = -1/2$ are closed for the capture, while the accurate results are quite different from this. The deficiency of the PR approximation is already seen from the fact that the term in the AC potential proportional to R^{-4} is positive which signals an inadequacy of the second-order approximation for the charge–permanent dipole interaction. If one simply ignores the behaviour of the PR potentials at smaller distances (say $R < 30$ a.u.), then the state with $m = +1/2$ should be counted as open for capture while that with $m = -1/2$ cannot be unambiguously qualified as open or closed. This indicates the caveat in using PR potentials even at low collision energies. We therefore calculated the capture rate coefficients with the help of accurate AC potentials. The plots of the reduced partial rate coefficients $\chi_{L,3/2,m}$ and the total reduced rate coefficient $\chi_{L,3/2}$ are presented in Fig. 5.

For $j > 3/2$, the shapes of AC potentials and state-specific rate coefficients become quite complicated and are not presented here, but the key features are given in Table 2. The plots for the total reduced rate coefficients $\chi_{L,j}(T)$ up to $j = 9/2$ are shown in Fig. 6. The highest value of j was chosen from the condition that the Hund coupling case a should still provide a good approximation to the rovibronic states.

We see that the $\chi_{L,j}(T)$, with $j > 3/2$, do not differ much among themselves, say for $T > 0.2$ K, but deviate notably from $\chi_{L,1/2}(T)$. In order to understand the tendency of $\chi_{L,j}(T)$ with increasing j, it is instructive to rewrite the PR potentials from eqn (4) as a function of the orientation angle β of the vector of the intrinsic angular momentum $\boldsymbol{j}$ with respect to the collision axis. Assuming $j \gg 1$ and using the quasiclassical

This journal is © the Owner Societies 2007

Phys. Chem. Chem. Phys., 2007, **9**, 1559–1567 | 1563

Table 2 Key features of the AC potentials for NO(X $^2\Pi_{1/2}$, j) + C$^+$ capture in different approximations (barrier heights $E_{j,m}^*$ are given as $E_{j,m}^*/k$ in Kelvin). The last column characterizes the accurate AC channels as open or closed for capture at T = 0.5 K. Italics refers to cases where the accurate behaviour differs from predictions for the charge–dipole interaction

j	m	Charge–dipole	Perturbed rotor	Accurate	Accurate, T = 0.2 K
1/2	+1/2	Open	Open	Open	Open
	−1/2	Closed	Barrier (0.800 K)	Barrier (0.657 K)	Closed
3/2	+3/2	Open	Open	Open	Open
	+1/2	Open	Closed	Open	Open
	−1/2	Closed	Closed	Barrier (3.00 K)	Closed
	−3/2	Closed	Barrier (1.55 K)	Barrier (1.12 K)	Closed
5/2	+5/2	Open	Open	Open	Open
	+3/2	Open	Open	Open	Open
	+1/2	Open	Closed	Open	Open
	−1/2	Closed	Closed	Barrier (0.00164 K)	*Open*
	−3/2	Closed	Barrier (0.224 K)	Barrier (2.57 K)	Closed
	−5/2	Closed	Barrier (3.51 K)	Barrier (2.08 K)	Closed
7/2	+7/2	Open	Barrier (0.239 K)	Barrier (0.0517 K)	Open
	+5/2	Open	Open	Open	Open
	+3/2	Open	Open	Open	Open
	+1/2	Open	Open	Open	Open
	−1/2	Closed	Barrier (0.00025 K)	Barrier (0.00025 K)	*Open*
	−3/2	Closed	Barrier (0.0160 K)	Barrier (0.0160 K)	*Open*
	−5/2	Closed	Barrier (0.602 K)	Barrier (2.63 K)	Closed
	−7/2	Closed	Barrier (7.16 K)	Barrier (3.62 K)	Closed
9/2	+9/2	Open	Barrier (2.85 K)	Barrier (1.30 K)	*Closed*
	+7/2	Open	Open	Open	Open
	+5/2	Open	Open	Open	Open
	+3/2	Open	Open	Open	Open
	+1/2	Open	Open	Open	Open
	−1/2	Closed	Barrier (0.000062 K)	Barrie (0.000062 K)	*Open*
	−3/2	Closed	Barrier (0.0028 K)	Barrier (0.0028 K)	*Open*
	−5/2	Closed	Barrier (0.0526 K)	Barrier (0.0526 K)	*Open*
	−7/2	Closed	Barrier (1.40 K)	Barrier (3.18 K)	Closed
	−9/2	Closed	Barrier (>10 K)	Barrier (5.72 K)	Closed

relation $\cos\beta = m\big/\sqrt{j+1/2}$, we get

$$V_{j,m}^{\text{PR}}(R)\Big|_{j\gg1} \equiv V_j^{\text{PR}}(R,\cos\beta)$$

$$= -\frac{|q|\boldsymbol{\mu}_\text{D}}{2(j+1/2)R^2}P_1(\cos\beta) - \frac{q\boldsymbol{Q}}{2R^3}P_2(\cos\beta) \qquad (19)$$

$$- \frac{q^2}{2R^4}\left[\boldsymbol{\alpha} + \frac{\boldsymbol{\mu}_\text{D}^2}{2B(j+1/2)^2}P_2(\cos\beta)\right]$$

Now, with a fixed value of β and increasing j, the first term decreases due to the diminishing projection of the dipole moment vector onto the $\boldsymbol{j}$ vector, and the last term decreases due to the lowering of the rotational polarization with increasing rotational energy. If we neglect the effect of the first and last term in eqn (19), we get the AC PR potentials that govern the capture of a classical quadrupole molecule by an ion. We therefore conclude that with increasing j, $\chi_{\text{L},j}(T)$ will converge to the classical capture rate coefficient for quadrupolar molecules. The convergence will be faster for higher temperatures since in these conditions the first term in eqn (19) plays a progressively minor role. Interestingly, $\chi_{\text{L},j}(T)$ for high j passes through a shallow minimum which is a typical feature of the capture rate coefficients of quadrupolar molecules.[14]

Two-temperature capture rate coefficients

Consider now a situation when the diatoms are taken from an ensemble with two canonical distributions, one with the translational temperature T_tr and the other with the rotational temperature T_rot. The reduced two-temperature average rate coefficient $\bar{\chi}_\text{L}(T_\text{tr}, T_\text{rot})$ is written as

$$\bar{\chi}_\text{L}(T_\text{tr}, T_\text{rot}) = \frac{1}{Z_\text{rot}(T_\text{rot})}\sum_{j\geq1/2}\chi_{\text{L}j}(T_\text{tr})(2j+1)$$
$$\times \exp\left(-\frac{B}{kT_\text{rot}}[j(j+1)-3/4]\right) \qquad (20)$$

where $Z_\text{rot}(T_\text{rot})$ is the rotational partition function

$$Z_\text{rot}(T_\text{rot}) = \sum_{j\geq1/2}(2j+1)\exp\left(-\frac{B}{kT_\text{rot}}[j(j+1)-3/4]\right) \qquad (21)$$

Fig. 7 shows the plots of $\bar{\chi}_\text{L}(T_\text{tr},T_\text{rot})$ for NO(X $^2\Pi_{1/2}$, thermal j) + C$^+$ capture as a function of the translational temperature T_tr and for different values of T_rot.

Expression (20), for NO + C$^+$ collisions, can be put into a simplified form by using the fact that all $\chi_{\text{L},j}(T_\text{tr})$ with $j > 3/2$ are approximately the same for $T_\text{tr} > 0.2$ K. If we replace $\chi_{\text{L},j}(T_\text{tr})$ with $j > 3/2$ in eqn (20) by $\chi_{\text{L},3/2}(T_\text{tr})$, we obtain a
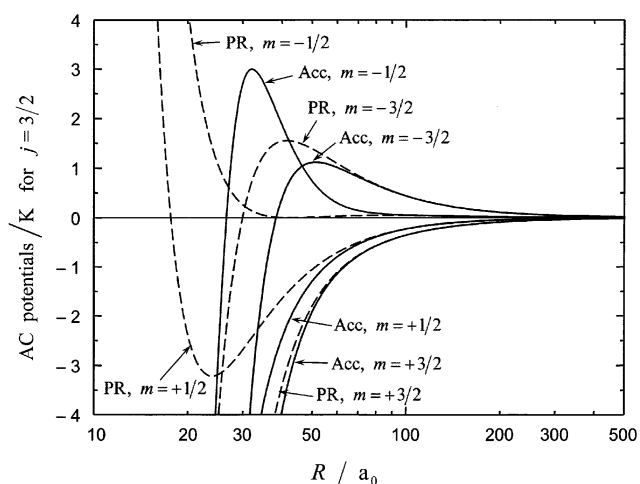
Fig. 4 Perturbed-rotor (dashed lines) and accurate (full lines) AC potentials for NO(X $^2\Pi_{1/2}$, $j = 3/2$) + positive ion.

useful interpolation formula which is valid within the temperature range $0.2 \leq T_{\mathrm{tr}}, T_{\mathrm{rot}} \leq 20$ K

$$\bar{\chi}_{\mathrm{L}}(T_{\mathrm{tr}}, T_{\mathrm{rot}}) \approx \tilde{\chi}_{\mathrm{L}}(T_{\mathrm{tr}}, T_{\mathrm{rot}}) = \frac{2}{Z_{\mathrm{rot}}(T_{\mathrm{rot}})} \chi_{\mathrm{L},1/2}(T_{\mathrm{tr}})$$
$$+ \left(1 - \frac{2}{Z_{\mathrm{rot}}(T_{\mathrm{rot}})}\right) \chi_{\mathrm{L},3/2}(T_{\mathrm{tr}}) \tag{22}$$

The performance of the simple expression (22) is demonstrated in Fig. 7.

5. Capture of NO(X $^2\Pi_{1/2}$) by C$^+$: comparison with experiment

Mazely and Smith[9] reported an experimental rate coefficient $1.99(\pm 25\%) \times 10^{-9}$ cm^3 molecule^{-1} s^{-1} for the charge-transfer reaction C$^+$ + NO $\rightarrow$ C + NO$^+$ at the translational temperature 0.6 K. Since this reaction is strongly exothermic, it is reasonable to assume that this rate coefficient corresponds
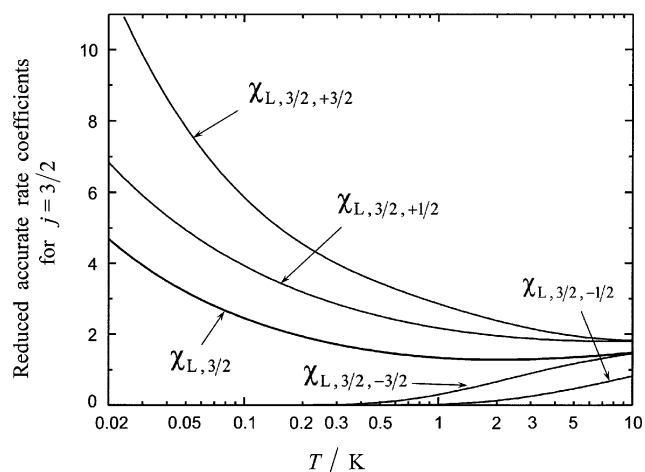

Fig. 5 Reduced partial (multplied by $2j + 1 = 4$) and total rate coefficients, $\chi_{\mathrm{L},j,m}(T)$ and $\chi_{\mathrm{L},j}(T)$ for NO(X $^2\Pi_{1/2}$, $j = 3/2$) + C$^+$ capture.
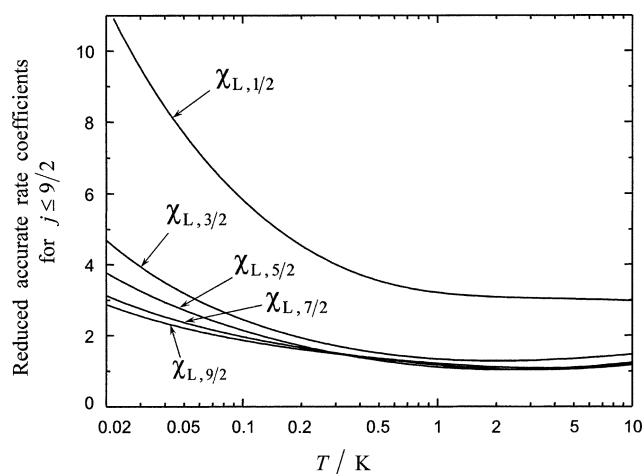

Fig. 6 Reduced total capture rate coefficients $\chi_{\mathrm{L},j}(T)$ for NO(X $^2\Pi_{1/2}$, j) + C$^+$ capture for $j = 1/2, 3/2, \ldots 9/2$.

to that of complex formation, *i.e.* to capture. The authors interpreted their findings in terms of the first-order charge–permanent dipole model that yielded the value of 1.7×10^{-9} cm^3 molecule^{-1} s^{-1}. This seemingly satisfactory correspondence was questioned by Wickham, Stoecklin and Clary (WSC),[7] who indicated the importance of the charge–induced dipole interaction (with the Langevin rate coefficient being equal to 1.046×10^{-9} cm^3 molecule^{-1} s^{-1}). The theoretical rate coefficient $k^{\mathrm{WSC}}(T_{\mathrm{tr}})$ which they suggested is identical to $k^{\mathrm{TPR}}_{1/2,+1/2}(T_{\mathrm{tr}})$, *viz.*,

$$k^{\mathrm{WSC}}(T_{\mathrm{tr}}) = \frac{1}{6} \boldsymbol{\mu}_{\mathrm{D}} q \sqrt{\frac{8\pi}{\mu k T_{\mathrm{tr}}}} + \pi q \sqrt{\frac{\boldsymbol{\alpha}}{\mu}} \tag{23}$$

which yields $k^{\mathrm{WSC}}(T_{\mathrm{tr}})|_{T_{\mathrm{tr}} = 0.6\ \mathrm{K}} = 2.38 \times 10^{-9}$ cm^3 molecule^{-1} s^{-1}. We see, however, from Fig. 3 that the value of $k^{\mathrm{TPR}}_{1/2,+1/2}(T_{\mathrm{tr}})$ is noticeably lower than its PR or the accurate counterparts. Thus, the accurate theoretical value of the rate coefficient for complex formation at $T_{\mathrm{tr}} = 0.6$ K and $j = 1/2$
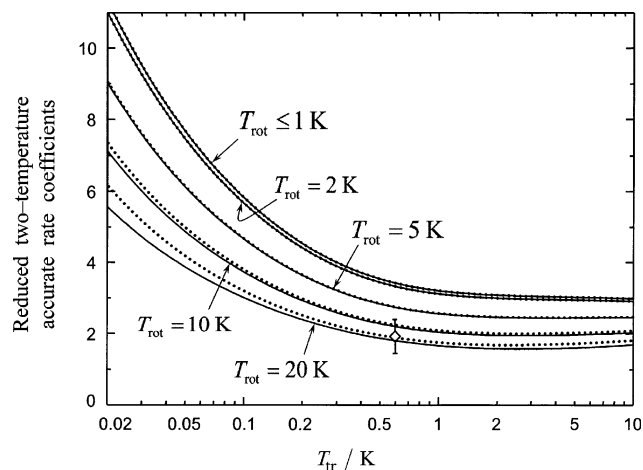

Fig. 7 Reduced two-temperature rate coefficients $\bar{\chi}_{\mathrm{L}}(T_{\mathrm{tr}}, T_{\mathrm{rot}})$ (full lines) and their approximate counterparts $\tilde{\chi}_{\mathrm{L}}(T_{\mathrm{tr}}, T_{\mathrm{rot}})$ (dashed lines) for NO(X $^2\Pi_{1/2}$, all j) + C$^+$ capture *vs.* translational temperature T_{tr} for different values of the rotational temperature T_{rot}. The symbol with error bars gives the experimental data from ref. 7.

This journal is © the Owner Societies 2007

Phys. Chem. Chem. Phys., 2007, **9**, 1559–1567 | 1565

turns out to be substantially higher than the experimental value (3.58×10^{-9} cm³ molecule⁻¹ s⁻¹ *vs.* 1.99×10^{-9} cm³ molecule⁻¹ s⁻¹). One of the reasons for this difference is the participation of rotationally excited molecules in the capture event. Indeed, Mazely and Smith[9] estimated the rotational temperature to be around 20 K. The value of the two-temperature rate coefficient $k(T_{tr}, T_{rot})$ as recovered from Fig. 7 for these two temperatures is 1.88×10^{-9} cm³ molecule⁻¹ s⁻¹ which agrees with the experimental value within the stated experimental errors. Yet, there is still a caveat in the comparison of the theoretical capture rate coefficient with the experimental value coefficient because not all electronic states of the complex that arise from electronic states of the reagents need to participate in the charge exchange. Since both reagents are in doublet states, $C^+(^2P) + NO(^2\Pi)$, there arise triplet and singlet states of the complex. On the other hand, the electronic states of the products that correlate with $C(^3P) + NO^+(^1\Sigma)$ fragments are triplets. If we assume that singlet states do not lead to reaction, the theoretical rate constant should be multiplied by an electronic statistical factor $g = g_{el}3/4$. Decrease of our theoretical value by a factor of 3/4 brings it down to the lowest possible experimental value which raises the interesting question whether intersystem crossing in the complex also allows the singlet states to participate fully in the energy redistribution in the complex.

Conclusion

The capture of $NO(X\ ^2\Pi_{1/2}, j)$ in a specific rotational state by a C^+ ion within the temperature range 0.02–20 K occurs in the regime where the collisions are adiabatic with respect to rotational and fine-structure transitions and sudden with respect to transitions between Λ doubling and hyperfine structure states. Therefore, the latter can be ignored in the capture dynamics, and the rate coefficients can be calculated within the adiabatic channel approach. The characteristic features of the AC potentials for this system are a small dipole moment and a small rotational constant of NO. The former suggests a strong contribution of charge–quadrupole and charge–induced dipole terms beyond the leading first-order charge–dipole term, while the latter implies an earlier breakdown of the weak-field (*i.e.* perturbed rotor) approximation. Both features manifest themselves in the temperature dependence of the state-specific rate coefficients. Purely attractive adiabatic channels lead to partial rate coefficients that show negative temperature dependence and bridge the $T^{-1/2}$ dependence (from the first-order charge–dipole dependence at lower temperatures) with a nearly constant high-temperature asymptote determined by the charge–induced dipole and second-order charge–dipole interaction. The adiabatic channels with activation barriers lead to positive temperature dependences of the rate coefficient. The height of the potential barriers is determined by an interplay of different terms in the interaction potential, and their reliable estimate cannot be achieved within the perturbed rotor approximation. The passage from capture in the ground state ($j = 1/2$) to that in excited states ($j > 1/2$) marks a noticeable drop in the rate coefficients due to the progressively stronger averaging of the charge–dipole interaction by molecular rotation. As a result, the two-temperature capture rate coefficient $k(T_{tr}, T_{rot})$, that depends on transla-

tional, T_{tr}, and rotational, T_{rot}, temperatures of two Boltzmann sub-ensembles, is characterized by a negative dependence both on T_{tr}, and on T_{rot}. The theoretical value of $k(T_{tr}, T_{rot})$ agrees reasonably well with an experimental value for the conditions of the experiment at $T_{tr} = 0.6$ K, $T_{rot} = 20$ K. Thus, our treatment suggests a revision of earlier interpretations that persisted for more than a decade.[3,5]

In parallel to the numerical calculations of the rate coefficient with accurate adiabatic channel potentials, we have presented the results based on perturbed rotor approximation for the rotational state $j = 1/2$. This was done for the following reasons:

(i) In the PR approximation, the capture rate coefficient for $j = 1/2$ can be calculated analytically. Since the $j = 1/2$ rate coefficient, for the system studied, is in reasonable agreement with the accurate rate coefficient, and since the reasons for this are clear, the analytical expressions for the rate coefficient can be recommended for application to other systems (see section 3).

(ii) PR approximation allows one to foresee the incipient quantum effects that are associated with relative motion of the collision partners. It was shown that such quantum effects will manifest at much lower temperatures compared to those where another quantum effect, the Λ doubling phenomenon, becomes important. The specificity of the capture in different components of the Λ doublet is now under investigation in our group.[6]

(iii) PR approximation allows one to qualitatively understand the tendency of the temperature dependence of the rate coefficients for large j with increasing j (see section 4).

The bottleneck for numerical calculations (in terms of computational power) of the rate coefficients for our and other systems is determination of the accurate adiabatic channel potentials. Once the analytical expression for the interaction potential in eqn (1) is accepted, the construction of the AC potential matrix in the basis of free rotor functions is technically trivial since the matrix elements are expressed through the vector addition coefficients which can be supplied by variety of standard codes (*e.g.* Mathematica). A person who is quite inexperienced in numerical calculations can get results for other systems, since the subsequent calculation of the capture rate coefficients, given in the integral representation, presents no difficulty. Computational power needed for classical calculations is negligible compared to quantum solution of coupled channel capture equations. Of course, the latter approach is necessary at much lower temperature when one has to take into account quantum effects in the capture as well as nonadiabatic Coriolis coupling.[3] However, this also requires accounting for the Λ doubling phenomenon and hyperfine structure effects.

Acknowledgements

References

1 S. C. Althorpe and D. C. Clary, *Annu. Rev. Phys. Chem.*, 2003, **54**, 493–529.
2 E. E. Nikitin and J. Troe, *Phys. Chem. Chem. Phys.*, 2005, **7**, 1540–1551.

3 D. C. Clary and P. Henshaw, *Faraday Discuss. Chem. Soc.*, 1987, **84**, 333.
4 J. Troe, *Ber. Bunsen-Ges. Phys. Chem.*, 1995, **99**, 341.
5 J. D. Graybeal, *Molecular Spectroscopy*, McGraw-Hill, New York, 1988.
6 E. I. Dashevskaya, I. Litvin, E. E. Nikitin and J. Troe, to be published.
7 A. G. Wickham, T. S. Stoecklin and D. C. Clary, *J. Chem. Phys.*, 1992, **96**, 1053–1061.
8 J. Troe, *J. Chem. Phys.*, 1987, **87**, 2773–2780.
9 T. L. Mazely and M. A. Smith, *Chem. Phys. Lett.*, 1988, **144**, 563–569.
10 R. N. Zare, *Angular Momentum*, Wiley, New York, 1988.
11 M. Quack and J. Troe, *Statistical Adiabatic Channel Models*, in *Encyclopedia of Computational Chemistry*, ed. P. V. Schleyer, N. L. Allinger, T. Clark, J. Gasteiger and P. A. Kollmann, Wiley, New York, 1998, vol 4, p. 2708.
12 S. C. Smith and J. Troe, *J. Chem. Phys.*, 1992, **97**, 5451–5464.
13 E. I. Dashevskaya, I. Litvin, A. I. Maergoiz, E. E. Nikitin and J. Troe, *J. Chem. Phys.*, 2003, **118**, 7313–7320.
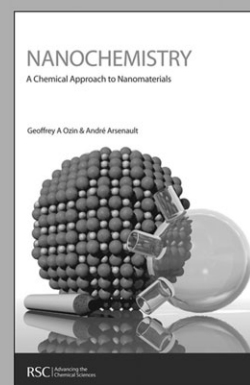14 E. I. Dashevskaya, I. Litvin, E. E. Nikitin and J. Troe, *J. Chem. Phys.*, 2005, **122**, 184311.

This journal is © the Owner Societies 2007

Phys. Chem. Chem. Phys., 2007, **9**, 1559–1567 | 1567